Available online at www.sciencedirect.com
ScienceDirect
Journal of Power Sources 160 (2006) 925–932
JOURNAL OF POWER SOURCES
www.elsevier.com/locate/jpowsour

Performance of a direct methanol fuel cell (DMFC) at low temperature: Cathode optimization

Tatyana V. Reshetenko, Hee-Tak Kim *, Hankyu Lee, Moonyup Jang, Ho-Jin Kweon

Samsung SDI Co. Ltd., 575 Shin-dong, Yeongtong-gu, Suwon-si, Gyeonggi-do 443-391, Republic of Korea

Received 6 January 2006; received in revised form 13 February 2006; accepted 13 February 2006
Available online 5 April 2006

Abstract

The effects of Pt loading, Nafion content in the cathode and membrane–electrode assembly (MEA) preparation techniques ($CCS_{cathode}/CCS_{anode}$ and $CCM_{cathode}/CCS_{anode}$) on the performance of MEAs for direct methanol fuel cells (DMFC) were studied. The MEA performance was analyzed with polarization curves, electrochemical impedance spectroscopy and scanning electron microscopy data. It was shown, that the cathode prepared by the catalyst coated membrane (CCM) method forms a mainly microporous and mesoporous structure, whereas the catalyst coated substrate (CCS) method generates macroporosity together with micropores and mesopores. The power density of the $CCM_{cathode}/CCS_{anode}$ typed MEAs strongly depends on the CCM-cathode composition: Pt loading and Nafion content in the cathode. Nafion (10.7 wt.%) was found to be an optimum for DMFC performance, and at this composition, the power density gradually increased with the Pt loading up to 6.0 mg cm^{-2}. At higher Nafion contents, a significant mass transfer limitation at high Pt loadings occurs. Comparing the CCM and CCS methods of the cathode fabrication, the latter revealed a higher power density, which reached 104 mW cm^{-2} at 0.4 V and 70 °C owing to the lack of significant mass transfer limitations. This behavior indicates that in addition to Pt loading and Nafion content, the cathode pore structure is critical to DMFC MEA performance.

Keywords: Direct methanol fuel cell; MEA preparation; Pt loading; Nafion content; EIS

1. Introduction

While the power efficiencies of polymer electrolyte membrane fuel cells (PEMFC) continue to show improvements, there are some problems with the use of hydrogen as the fuel. In this case, hydrogen has to be produced by reforming of hydrocarbons or supplied from a pressurized hydrogen tank. So there are increased engineering complexities and safety concerns. Therefore, it remains highly desirable to develop a fuel cell that would feed liquid fuel directly to the anode. From this point of view, the direct methanol fuel cell (DMFC) is a promising alternative to PEMFC for mobile fuel cell applications. Methanol has a number of advantages: (1) it is liquid and can be easily transported and stored; (2) it is relatively cheap; (3) the only products of methanol oxidation are water and CO_2, and there is no production of NO_x; (4) DMFC usually operates at low temperature, which significantly simplifies the engineering problems. Because of these advantages, DMFC is very attractive as a portable power source for small mobile devices such as cell phones and notebooks [1–5].

The anode and cathode reactions occurring in DMFC MEA are described below:

$$CH_3OH + H_2O \rightarrow CO_2 + 6H^+ + 6e^- \text{ (anode)}$$

$$\tfrac{3}{2}O_2 + 6H^+ + 6e^- \rightarrow 3H_2O \text{ (cathode)}$$

Even though the thermodynamic cell voltage corresponds to 1.21 V [6], DMFCs generally show a much lower open circuit voltage due methanol crossover [6,7]. In addition to methanol crossover, the low reaction rate is major huddle for performance improvement. Previous researchers have reported about developments of a membrane with low crossover [8–10], electrocatalysts for anode and cathode [7,3,11–13] and control of mass-transfer.

With respect to the catalyst layer, parameters such as catalyst loading and ionomer loading affect the MEA performance and have to be controlled [3,5,22,14–17]. Due to the slow kinetics, a high metal loading is necessary for acceptable performance, but this can result in increasing the DMFC cost. So, there is a need to find an optimum amount of Pt and Pt–Ru black catalysts for

* Corresponding author. Tel.: +82 31 210 7067; fax: +82 31 210 7374.
E-mail address: hee-tak.kim@samsung.com (H.-T. Kim).

0378-7753/$ – see front matter © 2006 Elsevier B.V. All rights reserved.
doi:10.1016/j.jpowsour.2006.02.058

effective DMFC operation. Some work on the effect of Pt black loading on the cathode have been reported [5,22,14–16]. Chen et al. [5,14] found that the maximum power density was achieved at a Pt loading of 6.2 mg cm^{-2}. On the other hand, it was reported that Pt black with content more than 4 mg cm^{-2} Pt did not affect the cell performance [16]. Though many papers have reported the effect of Pt content on the cathode, the optimum has been observed to be different.

It is well known that in order to provide proton transfer through the catalyst layer, an ionomer like Nafion is added to the catalyst layer [15,17,18]. Nafion enables the catalyst particles to be integrated with formation of three-dimensional network, and the optimum Nafion loading mostly depends on the catalyst type: black or supported [15,17,19,20]. It was shown that in the case of the Pt black, the optimum amount of the ionomer is 10.5 wt.% [15]. However, systematic and detailed studies of the Nafion loading effect appear to be not sufficient.

Another important issue for the MEA of a DMFC would be control of the MEA structure by fabrication procedure [21–24]. The catalyst layer can be formed on the surface of the diffusion layers having suitable polytetrafluoroethylene (PTFE) contents by various coating techniques. The catalyst coated diffusion layer is denoted as catalyst coated substrate (CCS) [25,26]. A five-layered MEA is prepared by hot-pressing the CCS anode and the CCS cathode with the proton conductive membrane. Wilson and Gottesfeld [27] suggested fabricating MEAs by a decal method, where catalytic ink is applied to a PTFE blank and subsequently transferred to the membrane. In another approach, the catalyst layer is formed by coating both sides of the membrane with the catalyst material, leading to three-layer structure, which is called as catalyst coated membrane (CCM) [25]. The textural properties of the catalyst layer are expected to vary with the MEA preparation method even when the catalyst ink and coating method are the same. For CCS, the catalyst layer would be coupled with a diffusion layer structure, however, for CCM, the gas diffusion layer does not affect the catalyst layer texture. Therefore, the effect of the MEA preparation method on performance may be analyzed considering the textural characteristics of the catalyst layer.

Considering the above-mentioned issues in catalyst layer design, our group has optimized a cathode structure with varying Pt loadings, Nafion contents and also the MEA preparation method. In this paper, we report how these design variables affect MEA performance and discuss the relationship between the cathode structure and MEA performance.

2. Experimental

2.1. MEA preparation

All investigated MEAs were prepared with Nafion 115 (DuPont). Pt–Ru (1:1) black (HiSpec 6000, Johnson Matthey) and Pt black (HiSpec 1000, Johnson Matthey) were used for the cathode and anode, respectively. We used carbon paper 10DA (SGL, Germany) which contains 20 wt.% PTFE and 10AA (SGL) which does not include any PTFE for the cathode and anode, respectively. On the surface of the anode diffusion layer, a 1:1 (w/w) mixture of carbon (Vulcan XC-72, Cabot) and PTFE (Dupont) dispersed in isopropyl alcohol was deposited to form a microporous carbon layer (MPL). The carbon loading level was controlled to be 0.26 mg cm^{-2}.

Catalyst inks, consisting of appropriate amount of unsupported catalysts, Nafion solution and isopropyl alcohol, were homogenized to disperse the catalyst. To prepare anode electrodes (CCS_{anode}) the anode ink was sprayed to the microporous carbon layer coated 10AA. The cathode electrodes ($CCM_{cathode}$) were produced by spraying of the cathode ink onto one side of Nafion 115. Also we produced a $CCS_{cathode}$ electrode by applying the catalyst ink to 10DA with MPL. The catalyst loading and the Nafion content of the electrodes studied in this work are listed in Table 1.

Morphological characteristics of the electrodes were investigated by scanning electron microscopy using JEOL JSM-6700F microscope.

Table 1
Main characteristics of the MEA samples

Sample	Anode				Cathode			
	Pt–Ru (mg cm^{-2})	MPL (mg cm^{-2})	Nafion (wt.%)	Carbon paper	Pt (mg cm^{-2})	MPL (mg cm^{-2})	Nafion (wt.%)	Carbon paper
CCM1c-20	6.28	0.26	10.7	SGL10AA	1.25	–	20.6	SGL10DA
CCM2c-20	6.28	0.26	10.7	SGL10AA	2.28	–	20.6	SGL10DA
CCM3c-20	6.28	0.26	10.7	SGL10AA	3.92	–	20.6	SGL10DA
CCM1c-16	6.28	0.26	10.7	SGL10AA	0.83	–	16.7	SGL10DA
CCM2c-16	6.28	0.26	10.7	SGL10AA	1.84	–	16.7	SGL10DA
CCM3c-16	6.28	0.26	10.7	SGL10AA	2.9	–	16.7	SGL10DA
CCM4c-16	6.28	0.26	10.7	SGL10AA	3.71	–	16.7	SGL10DA
CCM5c-16	6.28	0.26	10.7	SGL10AA	4.7	–	16.7	SGL10DA
CCM1c-10	6.1	0.26	10.7	SGL10AA	0.9	–	10.7	SGL10DA
CCM2c-10	6.1	0.26	10.7	SGL10AA	1.8	–	10.7	SGL10DA
CCM3c-10	6.1	0.26	10.7	SGL10AA	3.0	–	10.7	SGL10DA
CCM4c-10	6.1	0.26	10.7	SGL10AA	4.4	–	10.7	SGL10DA
CCM5c-10	6.1	0.26	10.7	SGL10AA	5.7	–	10.7	SGL10DA
CCS	6.28	0.26	10.7	SGL10AA	5.6	1.3	10.7	SGL10DA

In this paper, the ionomer content in the electrode was defined as follows:

$$\text{Nafion content (wt.\%)} = \frac{M_{\text{Nafion}}}{(M_{\text{catalyst}} + M_{\text{Nafion}})} \times 100\%,$$

where M_{Nafion} is the mass of dry ionomer and M_{catalyst} is the mass of bulk catalyst.

$CCM_{cathode}/CCS_{anode}$ MEAs were obtained by pressing the stack of 10DA, $CCM_{cathode}$ and CCS_{anode} at 125 °C and at 500 kgf cm^{-2}. $CCS_{cathode}/CCS_{anode}$ was prepared by pressing $CCS_{cathode}$ Nafion 115 and CCS_{anode} at the same conditions. The cell active area was 10 cm^2.

2.2. Electrochemical characterization

Polarization curves were recorded by Wonatech Fuel Cell Test Stations. The MEAs were sandwiched between two plates with serpentine flow channels. Electrical heaters and thermocouple were embedded in the plates for controlling the desired operating temperature. A pump was employed to supply 1 M aqueous methanol solution (anode stoichiometry = 3) to the anode. In the fuel cell mode the cathode was fed by air at atmospheric pressure (cathode stoichiometry = 3). The cell temperature was varied in the range 50–70 °C. As a preconditioning step, we operated the cell at 0.4 V and at 50 °C for 2 h, and then measured the *I–V* polarization curve. It was repeated for several days. We have found that the cell performance stabilized within three days. The *I–V* polarization curves presented here were measured after a 3-day preconditioning procedure.

Electrochemical impedance spectroscopy investigations were carried out using IM-6 (Zahner, Germany) at 50 °C in the frequency range from 100 kHz to 1 mHz. Impedances were measured under galvanostatic control of the cell. The amplitude of the sinusoidal voltage signal did not exceed 5 mV. In order to separate the anode and cathode impedances we recorded the anode impedance by supplying hydrogen and 1 M MeOH solution to the cathode and anode compartments, respectively [28,29]. In this configuration, the cathode acts as reversible hydrogen electrode. Since proton reduction at the cathode is much faster than methanol oxidation at anode, the impedance contribution from

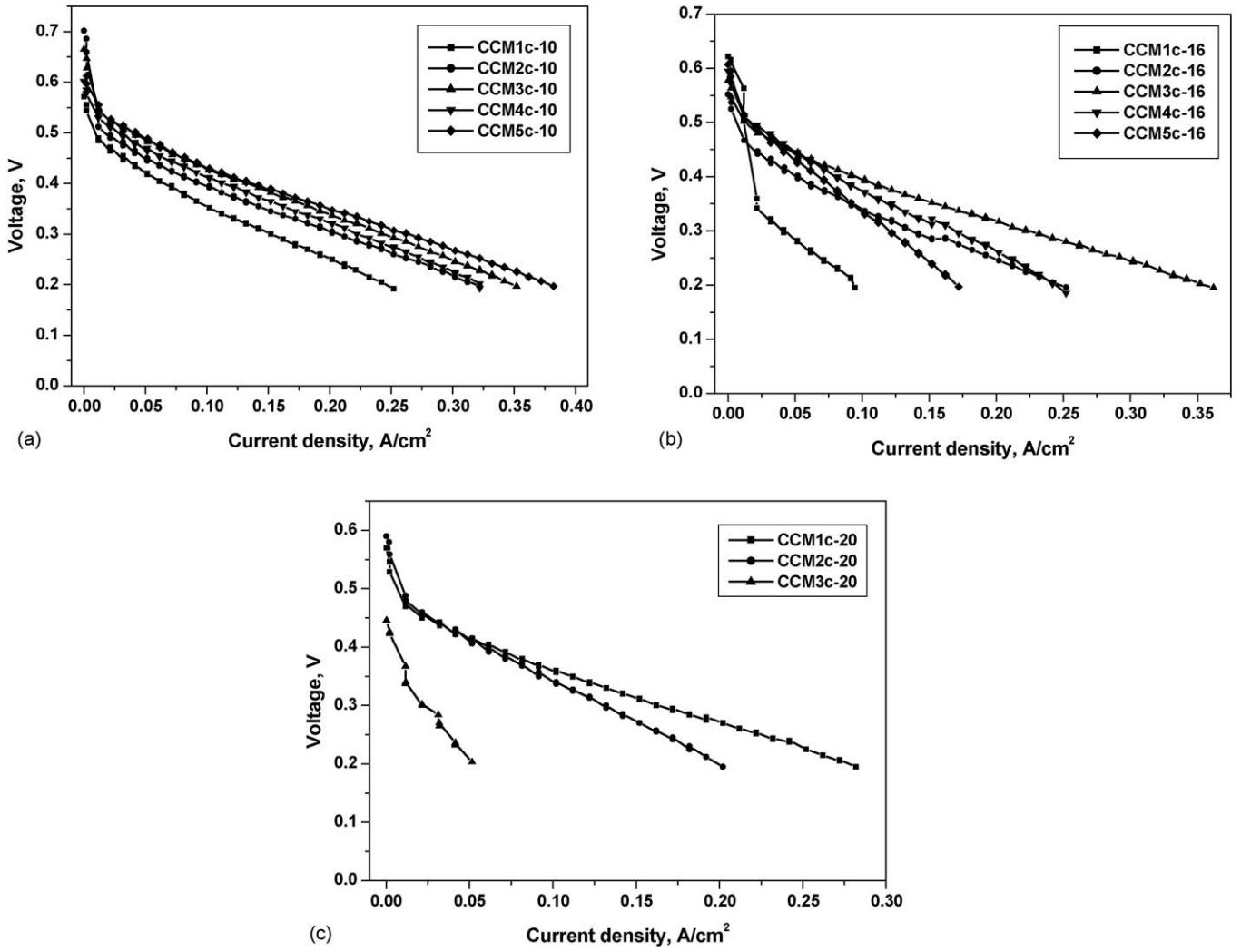

Fig. 1. Polarization curves for the samples with different cathode loadings (T = 50 °C, 1 M MeOH): (a) 10.7 wt.% Nafion, (b) 16.7 wt.% Nafion and (c) 20.6 wt.% Nafion.

the cathode can be neglected. The anode impedances are subtracted from the total cell impedances measured under air/1 M MeOH feed, resulting in the cathode impedance spectrum.

3. Results and discussions

3.1. Effect of the cathode composition

The current–voltage curves of the MEAs with 10.7, 16.7 and 20.6 wt.% Nafion content in the cathode layer and various Pt loadings are presented in Fig. 1a–c. The cell performance was found to increase as the Pt loading was increased from 0.9 to 5.7 mg cm^{-2} at 10.7 wt.% Nafion content in the cathode layer (Fig. 1a). This result is in good accordance with published data on the optimal platinum loading [14,16]. When the Nafion content was increased up to 16.7 wt.%, it showed different behavior (Fig. 1b). Inspections of the *I–V* curves showed that the current density increased with raising of the Pt content to 2.9 mg cm^{-2}, however, further increase of Pt loading resulted in a decrease of the current density at a cell voltages lower than 0.45 V. Polarization curves for samples containing 20.6 wt.% Nafion given in Fig. 1c show a maximum performance for the sample CCM1c-20 (1.25 mg cm^{-2}). The increase of Pt loading resulted in decrease of the cell performance especially in the high current density region. CCM1c-20 and CCM2c-20 did not show discernible differences at high voltages 0.4 V, however, they had a different power density in the high current density region. At the highest Pt loadings (CCM3c-20), there was a large over-potential over the entire voltage range.

The dependence of power density at 0.4 V on Pt loading is presented in Fig. 2a and b and Table 2. The power density of the samples was found to decrease as the Nafion content in the cathode layer increases at a catalyst loading higher than about 2.0 mg cm^{-2}, which is in agreement with the published results [15,17] and close to the data obtained for the PEMFC [18,30–32]. For electrodes with a 10.7, 16.7 and 20.6 wt.% Nafion content, the maximum performances are observed at 1.25, 2.9 and 5.7 mg cm^{-2} Pt, respectively. The comparison of

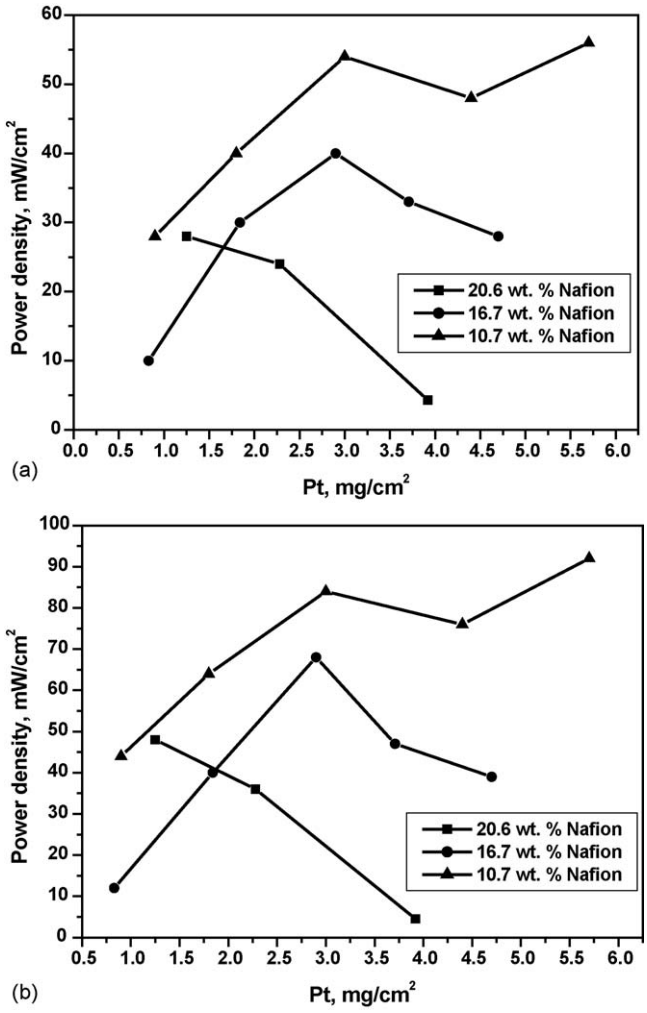

Fig. 2. The dependence between power density at 0.4 V and Pt loading at different Nafion contents: (a) $T = 50\,^{\circ}C$ and (b) $T = 70\,^{\circ}C$.

Fig. 2a and b shows that optimum Nafion content and Pt loading were not changed with the operation temperature. The maximum power density attainable in this optimization was 56 mW cm^{-2} at 50 °C and 92 mW cm^{-2} at 70 °C for CCM5c-10.

Table 2
The power density of the studied MEA samples

Sample	Pt–Ru (mg cm^{-2})	Pt (mg cm^{-2})	Nafion (cathode) (wt.%)	Power density at 0.4 V, mW cm^{-2}		
				50 °C	60 °C	70 °C
CCM1c-20	6.28	1.25	20.6	28	40	48
CCM2c-20	6.28	2.28	20.6	24	33	36
CCM3c-20	6.28	3.92	20.6	4	5	5
CCM1c-16	6.28	0.83	16.7	10	11	12
CCM2c-16	6.28	1.84	16.7	30	33	40
CCM3c-16	6.28	2.9	16.7	40	56	68
CCM4c-16	6.28	3.71	16.7	33	44	47
CCM5c-16	6.28	4.7	16.7	28	36	39
CCM1c-10	6.1	0.9	10.7	28	37	44
CCM2c-10	6.1	1.8	10.7	40	53	64
CCM3c-10	6.1	3.0	10.7	54	72	84
CCM4c-10	6.1	4.4	10.7	48	64	76
CCM5c-10	6.1	5.7	10.7	56	76	92
CCS	6.28	5.6	10.7	68	88	104

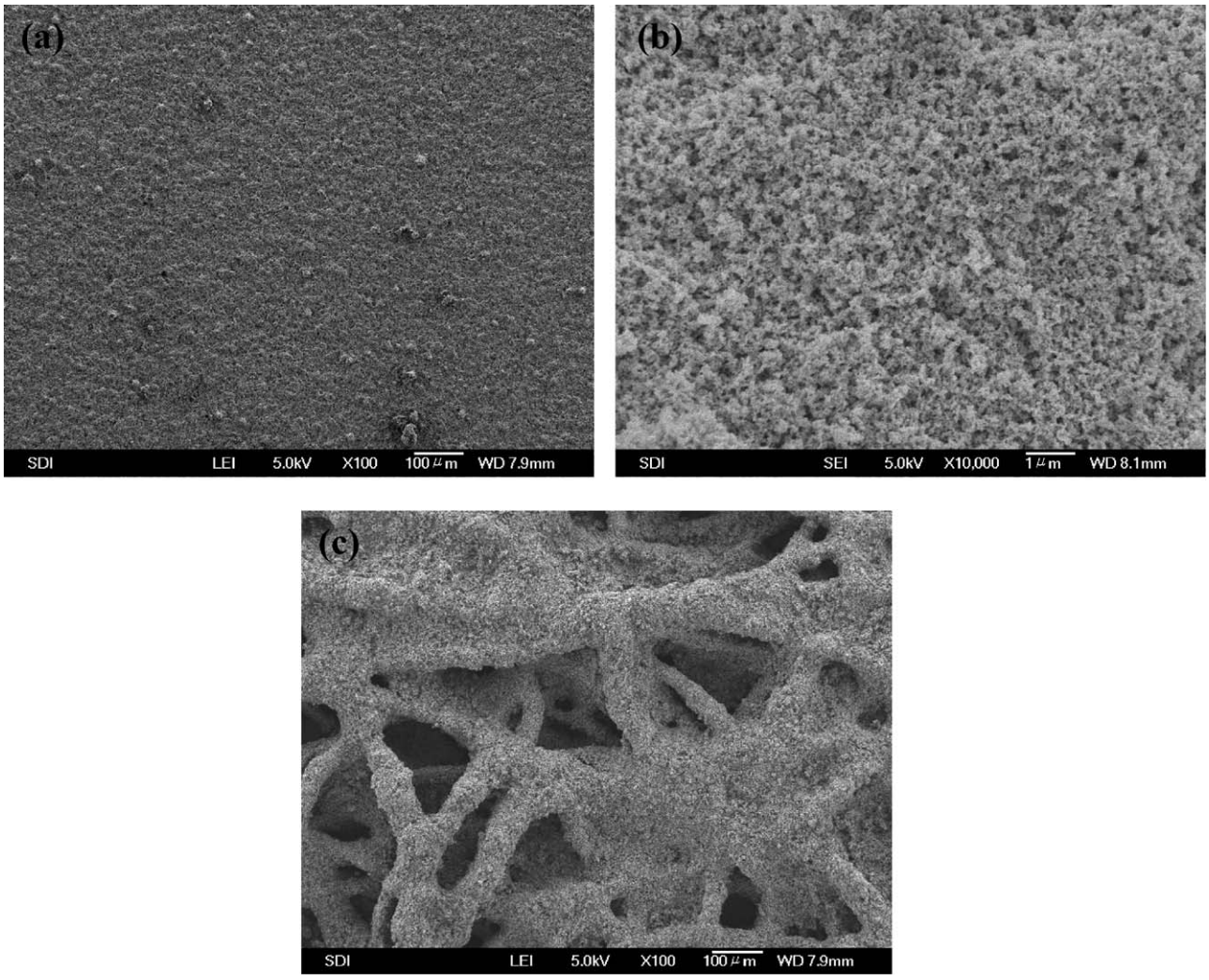

Fig. 3. SEM images of the electrodes: (a and b) CCM cathode and (c) CCS cathode (Pt black catalyst).

Introduction of Nafion into the electrode can extend the three-phase contact between reactant gases, electrolyte and the catalyst surface and make the layer more active in three dimensions since protons can move throughout the entire layer, which would improve the cell performance. It was shown for PEMFCs that the specific ionic conductivity of the catalyst layer is approximately proportional to the volume fraction of Nafion, and ionic conductivity limits the active layer thickness to 20–25 μm [33]. Antolini et al. [18] had assumed an empirical relationship to calculate the optimal Nafion loading for PEMFC in the electrode layer in the case of Pt/C supported catalyst.

The structure of the electrode layer is composed of Pt agglomerates coated by a Nafion film. It was reported that the catalytic layer usually has a dual pore distribution: the smaller pores (primary pores) have been attributed to pores in the agglomerates and the larger pores (secondary pores) are located between the agglomerates [34]. According to Uchida's suggestion, the Nafion should be localized in the secondary pores and coat Pt agglomerates [18,35]. In this model we can expect that the reaction of oxygen (electroreduction) would be controlled by the following transport processes: (1) oxygen diffusion into the

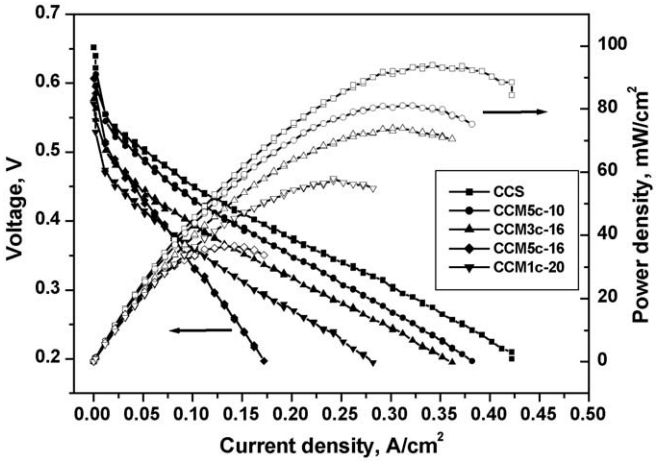

Fig. 4. Effect of Pt and Nafion loadings on performance of DMFC tested with 1 M MeOH at 50 °C.

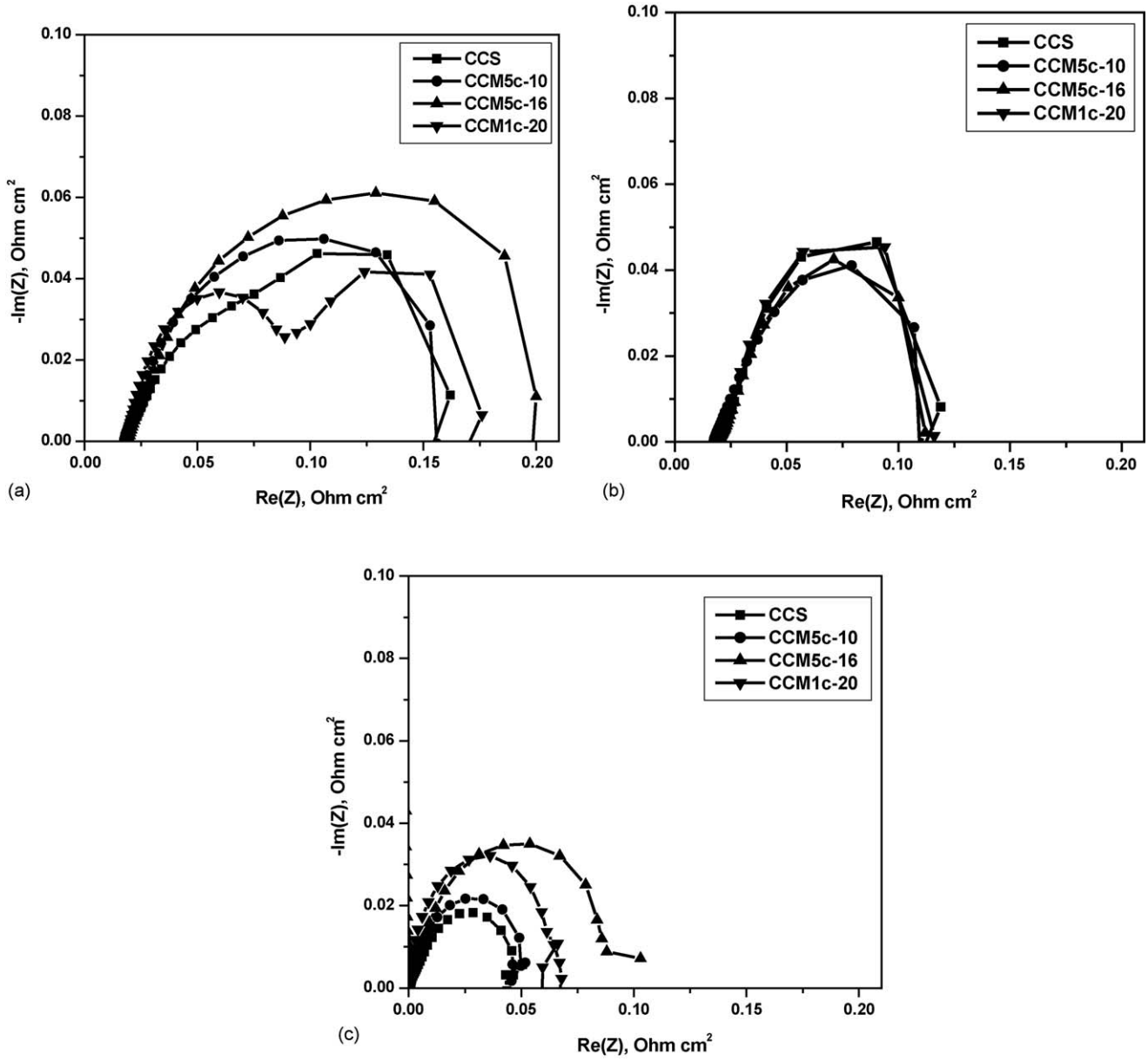

Fig. 5. Nyquist plots of MEAs under the study ($T = 50\,^{\circ}C$, $i = 90\,mA\,cm^{-2}$): (a) total, (b) anode and (c) cathode impedance.

pore space of the electrode and dissolution into Nafion; (2) oxygen diffusion through Nafion layer; (3) proton transfer in the Nafion layer. So, a low Nafion content (less than 10 wt.%) is not desirable since it could not ensure a good contact between the catalyst, electrolyte and reagents, so integrity of the catalyst layer and membrane and the proton conductivity would be not sufficient. At high ionomer loadings, the proton conductivity is enhanced, but it should be expected to limit catalyst utilization due to formation of a thick Nafion layer on the catalyst surface therefore the electroconductivity of the Pt layer would decrease [15,18,19]. We observed that the mechanical integrity of the catalyst layer is not sufficient below a 10.7 wt.% Nafion content. It means that the incorporated Nafion cannot properly bind catalyst particles. At 16.7 and 20.6 wt.% Nafion content, the decrease of power density at a high loading level indicates that a thick Nafion layer limits catalyst utilization in spite of enhanced proton conductivity in the catalyst layer. According to our results, it can be concluded that the 10.7 wt.% of Nafion content is acceptable for proton transfer within the catalyst layer without limiting oxygen diffusion.

3.2. *Effect of cathode structure*

According to the scanning electron microscopy images (Fig. 3) it seems reasonable that the CCM method of MEA manufacturing predominantly provides a microporous and mesoporous structure for the electrode layer, whereas the CCS technique produces a macroporous electrode. It should be noted that pores with an effective size up to 2 nm are called micropores; mesopores correspond to pore diameters in the range of 2–100 nm; whereas macropores are more than 100 nm [36]. The effective pore size is the maximum diameter of a circle that can

Table 3
EIS characterization of the MEAs ($T = 50\,^{\circ}C$, $i = 90\,mA\,cm^{-2}$)

Parameter	CCM5c-10	CCM5c-16	CCM1c-20	CCS
R_S ($m\Omega\,cm^2$)	17.5	19.7	18.7	18.4
OCV (V)	0.602	0.595	0.610	0.655
Total (V)	0.425	0.363	0.408	0.472
Anode (V)	0.378	0.384	0.362	0.361
Cathode (V)	0.803	0.747	0.770	0.833

R_S, ohmic resistance; OCV, open circuit voltage.

be fitted into a plane section of a randomly shaped pore. It is reasonable to suggest that the morphological characteristics of the CCS catalyst layer are affected by that of the diffusion layer. The 100 μm sized large pores shown in the $CCS_{cathode}$ correspond to the pores of the diffusion layer. Since mass transfer processes would play a significant importance and seem to be dominant on the cathode electrode, as deduced from Fig. 2, it is necessary to study the effect of the cathode texture on the MEA performance. We compared the CCS cathode and the CCM5c-10 cathode, which showed a maximum performance in the previous section, to elucidate the effect of the large pores on MEA performance. These two cathodes are the same in Nafion content and Pt loading. Comparison of the polarization curves for the CCM5c-10 and CCS MEA reveals that the CCS demonstrates a high performance over the whole current density region (Fig. 4 and Table 2). The power density of the CCS MEA reaches $68\,mW\,cm^{-2}$ at $50\,^{\circ}C$ and exceeds the power density of the $CCM_{cathode}$ MEAs. In order to explain such behavior, we performed electrochemical impedance analysis for few selected MEAs including CCM5c-10 and CCS.

Fig. 5a–c shows the Nyquist plots of the total, anode and cathode impedance with various Nafion contents in the cathode layer measured at $50\,^{\circ}C$ and current density of $90\,mA\,cm^{-2}$. Table 3 presents the main electrochemical parameters detected from the measurements. It can be seen that the total impedance curves for the studied samples are made up of approximately two semicircles which correspond to the oxygen reduction reaction and the methanol oxidation reaction. The larger semicircle approximately relates to the larger reaction resistance. Comparison of the anode impedance curves reveals that anode resistances are very close (Fig. 5b), which is reasonable because the anode composition was the same in these MEAs. The main differences are observed in the cathode impedances (Fig. 5c). The sizes of the semicircle in cathode impedance plot are in good agreement with the power density. The larger the size of the semicircle, the lower the power density at $90\,mA\,cm^{-2}$. The sample CCS shows the smallest semicircle among the MEAs, which can explain its highest power density.

Based on the impedance spectroscopy data (Fig. 5c) it can be seen that oxygen electroreduction rate is low for the samples with a high Nafion loading (16.7 and 20.6 wt.%). In this case, the ionomer in the cathode acts as an electrical resistance and a barrier to mass transfer either by retarding the oxygen access to the catalyst surface or by blocking desorption of products of the electroreduction, desspite the surface of the cathode layer being not very dense (Fig. 3a and b). The slight increase in ohmic resistance with increase of Nafion content (see Table 3) could result from increased electronic resistance of the catalyst layer. However, the difference in ohmic resistance is quite small compared to the difference in cathode reaction resistance. Thus, it is reasonable that the performance change with Nafion content mainly comes from decreased mass transfer.

The smaller cathode resistance for CCS compared to that for CCM5c-10 also suggests the importance of oxygen transfer in the catalyst layer. Even though microporosity and mesoporosity are the same between the two MEAs, the existence of large pores, which could act as a transport pores for the reagent, significantly accelerates the oxygen reduction reaction. The comparison of OCVs also supports this consideration. The OCV values for CCS and CCM5c-10 was 0.655 and 0.602 V, respectively. Since the same anode and membrane were employed, the amount of methanol crossover should be the same. The oxygen in the cathode is continuously consumed due to methanol oxidation, and the relative rate of oxygen diffusion through catalyst layer over oxygen consumption determines equilibrium oxygen concentration at catalyst surface. Thus, the higher OCV for CCS would indicate faster oxygen transfer to the catalyst surface.

4. Conclusions

In the present paper, the effects of the catalyst layer composition and the MEA preparation technique ($CCS_{cathode}$/CCS_{anode} and $CCM_{cathode}$/CCS_{anode}) on the performance of a DMFC were studied. It was shown, that the CCM method for electrode manufacturing generates a microporous and mesoporous texture, whereas the CCS method ensures formation of macroporosity. The performance of the combined $CCM_{cathode}$/CCS_{anode} MEAs depends on the $CCM_{cathode}$ composition: Pt loading and Nafion content in the cathode. For the CCM designed cathode, the optimal Nafion loading in the cathode layer is 10.7 wt.%, which is a reasonable balance between ionic and oxygen transfers. On the other hand, the performance of the $CCS_{cathode}$, which includes large as well as small pores, reached $104\,mW\,cm^{-2}$, due to the enhanced oxygen transport through the macropores. This result indicates that the pore structure should be carefully designed for the $CCM_{cathode}$ where only small pores predominate.

References

[1] H. Dohle, H. Schmitz, T. Bewer, J. Mergel, D. Stolten, J. Power Sources 106 (2002) 313.

[2] A.K. Shukla, A.S. Arico, V. Antonucci, Renew. Sust. Energy Rev. 5 (2001) 137.
[3] A.S. Arico, S. Srinivasan, V. Antonucci, Fuel Cells 1 (2001) 133.
[4] A. Blum, T. Duvdevani, M. Philosoph, N. Rudoy, E. Peled, J. Power Sources 117 (2003) 22.
[5] C.Y. Chen, P. Yang, Y.S. Lee, U.F. Lin, J. Power Sources 141 (2005) 24.
[6] W. Vielstich, A. Lamm, H.A. Gasteiger (Eds.), Handbook of Fuel Cells, vol. 1, John Wiley & Sons Ltd., 2002, pp. 305–308.
[7] M.P. Hogarth, T.R. Ralph, Platinum Met. Rev. 46 (2002) 146.
[8] M. Walker, K.M. Baumgärteher, M. Kaiser, J. Kerres, A. Ullrich, E. Rauchle, J. Appl. Polym. Sci. 74 (1999) 67.
[9] J.A. Kerres, J. Membr. Sci. 185 (2001) 3.
[10] V. Baglio, A.S. Arico, A. DiBlasi, V. Antonucci, P.L. Antonucci, S. Licoccia, E. Traversa, F. Serraino Fiory, Electrochem. Acta 50 (2005) 1241.
[11] A. Hamnett, Catal. Today 38 (1997) 445.
[12] V. Rao, P.A. Simonov, E.R. Savinova, G.V. Plaksin, S.V. Cherepanova, G.N. Kryukova, U. Stimming, J. Power Sources 145 (2005) 178.
[13] A.S. Arico, C. Creti, H. Kim, R. Mantegna, N. Giordano, V. Antonucci, J. Electrochem. Soc. 143 (1996) 3950.
[14] C.Y. Chen, P. Yang, J. Power Sources 123 (2003) 37.
[15] S.C. Thomas, X. Ren, S. Gottesfeld, J. Electrochem. Soc. 146 (1999) 4354.
[16] V. Gogel, T. Frey, Z. Yongsheng, K.A. Friedrich, L. Jörissen, J. Garche, J. Power Sources 127 (2004) 172.
[17] K. Furukawa, K. Okajima, M. Sudoh, J. Power Sources 139 (2005) 9.
[18] E. Antolini, L. Giorgi, A. Pozio, E. Passalacqua, J. Power Sources 77 (1999) 136.
[19] J.-H. Kim, H.Y. Ha, I.-H. Oh, S.-A. Hong, H.N. Kim, H.-I. Lee, Electrochem. Acta 50 (2004) 801.
[20] X. Zhao, X. Fan, S. Wang, S. Yang, B. Yi, Q. Xin, G. Sun, Int. J. Hydrogen Energy 30 (2005) 1003.
[21] W. Vielstich, A. Lamm, H.A. Gasteiger (Eds.), Handbook of Fuel Cells, vol. 4, John Wiley & Sons, 2002.
[22] Z. Wei, S. Wang, B. Yi, J. Liu, L. Chen, W. Zhou, W. Li, Q. Xin, J. Power Sources 106 (2002) 364.
[23] A. Lindermeir, G. Rosenthal, U. Kunz, U. Hoffman, J. Power Sources 129 (2004) 180.
[24] S.Q. Song, Z.X. Liang, W.J. Zhou, G.Q. Sun, Q. Xin, V. Stergiopoulos, P. Tsiakaras, J. Power Sources 145 (2005) 495.
[25] W. Vielstich, A. Lamm, H.A. Gasteiger (Eds.), Handbook of Fuel Cells, vol. 3, John Wiley & Sons, 2002.
[26] E.A. Ticianelli, C.D. Derouin, A. Redondo, S. Srinivasan, J. Electrochem. Soc. 135 (1988) 2209.
[27] W.S. Wilson, S. Gottesfeld, J. Electrochem. Soc. 139 (1992) L28.
[28] J.T. Mueller, P.M. Urban, J. Power Sources 75 (1998) 139.
[29] J.T. Müller, P.M. Urban, W.F. Hölderich, J. Power Sources 84 (1999) 364.
[30] E. Passalacqua, F. Lufrano, G. Squadrio, A. Patti, L. Giorgi, Electrochim. Acta 46 (2001) 799.
[31] Z. Qi, A. Kaufman, J. Power Sources 113 (2003) 37.
[32] G. Sasikumar, J.W. Ihm, H. Ryu, J. Power Sources 132 (2004) 11.
[33] C. Boyer, S. Gambruzev, O. Velev, S. Srinivasan, A.J. Appleby, Electrochim. Acta 43 (1998) 3703.
[34] M. Uchida, Y. Aoyama, N. Eda, A. Ohta, J. Electrochem. Soc. 142 (1995) 4143.
[35] M. Uchida, Y. Fukuoka, Y. Sugawara, N. Eda, A. Ohra, J. Electrochem. Soc. 143 (1996) 2245.
[36] S.J. Gregg, K.S.V. Sing, Adsorption, Surface Area and Porosity, second ed., Academic Press, London, 1982.